https://doi.org/10.5194/egusphere-2022-340
Preprint. Discussion started: 12 July 2022

Resolving the water budget of a complex carbonate basin in Central Italy with parsimonious modelling solutions

Shima Azimi[1,2], Christian Massari[2], Giuseppe Formetta[1], Silvia Barbetta[2], Alberto Tazioli[3], Davide Fronzi[3], Sara Modanesi[2], Angelica Tarpanelli[2], and Riccardo Rigon[1]

[1]University of Trento, Department of Civil, Environmental and Mechanical Engineering, Center Agriculture, Food and Environment (C3A), Trento, Italy
[2]National Research Council (CNR), Research Institute for Geo-Hydrological Protection, Perugia, Italy
[3]Università Politecnica delle Marche, Department of SIMAU, Ancona, Italy

Correspondence: Riccardo Rigon (Riccardo.rigon@unitn.it)

Abstract.

Placed at the center of the Mediterranean, the Apennines chains provide a critical water supply for people living in the Italian Peninsula. Yet, the quantification of water resources in this region is challenging given that the different components of the water cycles (i.e., snowmelt, evapotranspiration, and subsurface water recharge) are highly variable in space and time due to the specificity of the climate, the reforestation trend, and the complex landscapes and geology. In this study, we investigated the challenging hydrological river regime of a complex carbonate basin with significant external (and partially karst) groundwater contribution – the Upper Nera basin – affected by recent important seismic sequences.

When dealing with such type of basins, the generic approach to delineate the basin boundaries based on the geomorphology of the area can lead to questionable results potentially yielding significant water budget imbalances. Therefore, both (hydro)geological and hydrological features have to be considered for understanding the challenging hydrological behavior of these basins.

Here we proposed a specific analysis of precipitation-runoff time series corroborated with hydro-geological survey to obtain information on the basin response time and the real contribution area of the basin. Then, we integrated this information within the structure of a hydrological model (i.e., the Geoframe modelling system) by using a parsimonious type of approach to improve the description of the different components of the water balance with a specific focus on external groundwater recharge. We validated the model against in situ discharge observations and with remote sensing information of evapotranspiration and snow. Since these two variables (snow cover and evapotranspiration) play the crucial role in correct estimation of water balance in the basin, in this study we additionally focused on that.

We show that the model (tested with several hydrological signatures and a new conceptual evaluation based on an empirical probability function) performs relatively well in reproducing the different water balance components (including remotely sensed evapotranspiration and snow) and that the upper river basin is significantly impacted by carbonate rock river discharge (i.e., up to 85% in proportion to the total discharge for some stations) coming from outside the geomorphological boundary of the basin. Yet, the groundwater recharge effects on the river, gradually attenuates at the outlet of the basin (Visso station).

https://doi.org/10.5194/egusphere-2022-340
Preprint. Discussion started: 12 July 2022

Keywords: *Fissured and Karst basin; GEoframe-Newage modeling system; Spatial Snow Cover Variation; Actual Evapotranspiration; Correlation Analysis; Empirical error score.*

1 Introduction

Karst landscapes cover approximately 15 percent of the Earth surface and provide a challenge for the hydrologists. The topography of the karst area forms during tens of thousands of years creating different features such as karren, dolines, swallow holes. The excess of precipitation could create the networks of open fractures, conduits, and caves where water flows relatively fast into the springs and causes the peculiar response to the precipitation-runoff process of the system. In some geological systems, karst subterranean environments are also coupled with widespread fissures, fractures and porous medium especially in carbonate rocks; in these cases groundwater flow is often characterized by different flowpaths superimposed and occurring even in the same aquifer and/or hydro-structure (Kiraly et al. (1995)).

Both observations (using tracer's theory) and time series analysis are useful tools for detecting the zones involving groundwater flux by karst and fissures, and investigating the response of such complex systems. Generally, in the first approach the artificial tracer is introduced into the sinkholes and traces of the tracer are sought far away from it in the surrounding areas Hartmann et al. (2014), Zhang et al. (2021) and Nanni et al. (2020). The techniques using the correlation between precipitation and discharge can also provide informative details on the groundwater behavior, specifically in case of the lack of field information about the water circulation in the basin. For instance, Fiorillo and Doglioni (2010) carried a cross-correlation analysis to cope with the time that water needs to flow through the karst and fissured aquifers. Another useful method of the second approach has been borrowed from applied economics (Kristoufek, 2014, 2015) by Giani et al. (2021) for successfully estimating the basin characteristic response time of the hydrographs concerning the precipitation.

The analysis of the precipitation-runoff process of a basin is usually considered as straightforward task that can be accomplished equally well by a variety of models. However, hydrological simulations in basins, where groundwater contribution from outside the basin boundaries is significant (and also potentially sourced by karst landscapes), have been challenging issues for hydrologists during the last decade (Fan (2019); Kourgialas et al. (2010)). Indeed, delineating the watershed automatically from Digital Elevation Models (DEMS) for these basins, can lead to extraction of wrong flow paths and a basin area. In these cases, the information from geological surveys and tracer tests can help to circumvent this problem but is also not straightforward to embody in classical hydrological models.

For taking into account the external groundwater contributions to the basin (especially happening over karst-type of basins), different approaches have been applied: (1) distributed, process-based models (e.g., Rooji (2020), Hartmann et al. (2014)), which are based on solving groundwater partial differential equations along unknown and buried path; (2) black box, machine learning based, models in which all the details about the structure of the aquifer and hydrodynamics parameters are not needed (e.g., Tapoglou et al. (2014) and Castilla-Rho et al. (2015)), (3) lumped models, i.e. with sets of ordinary differential equations (ODEs) which conceptualize the physical processes at the scale of the whole karst system without modelling spatial variability explicitly as in Hartmann et al. (2014), Mazzilli et al. (2019), Rimmer and Hartmann (2012), Butscher and Huggenberger

https://doi.org/10.5194/egusphere-2022-340
Preprint. Discussion started: 12 July 2022

(2008) and Tritz et al. (2011). In the latter, different water budget components of the contributing area including internal and external runoff (Jukic and Denić-Jukić (2009)), epikarst storage and flow concentration (Tritz et al. (2011)), groundwater flow and storage in conduits (Butscher and Huggenberger (2008)) have been investigated. In both cases of using either process-based modelling or lumped models, the problem of parameter identification remains an important issue.

In this study, we explored the complex hydrological behavior of the upper Nera basin (central Italy), using a parsimonious strategy based on a system of ODEs and simulated the hydrological behavior close to Visso, Castelsantangelo (CSA), and Ussita sites (see Fig. 1). The basin is characterized by carbonate rocks showing both karst and small fissures features (Nanni et al. (2020)). Due to the impossibility of fully characterizing the complex groundwater system (that significantly impacts the basin hydrology), a physically-based coupled surface-groundwater modelling exercise is unfeasible thus we show that relatively good results can be still obtained by using a few experimental data and time series analysis. This has significant and general implications for the modelling of catchments characterized by significant external groundwater contributions. In particular, to calculate the partitioning between precipitation and runoff as well as the response time characteristic of the basin, we used the information derived from the rainfall-discharge correlation analysis. Our research experiment is organized as follows:

1. We show that using only shape and topography information to define basin area can lead to a considerable water budget inbalance.
2. After having calculated the real contributing area and assessed the basin time response by time series analysis and tracer test information, we show how the flexibility of the GEOframe-Newage tools embody this information to estimate water budget components.
3. We examined the suitability of the new model structure obtained by combining a system of ODEs with the GEoframe-Newage modeling system in estimating the basin hydrological behavior by using in situ discharge observations and remote sensing data of ET and snow as validation data.
4. We determined how the carbonate rocks discharge affects the river regime in the Upper Nera River basin, as well, its proportion relative to the other components of the hydrological cycle (i.e., evaporation, storage, and surface water).

Besides the scientific interest, knowing the discharge of the upper Nera River is essential because it is a regional water resource for multipurpose water supplies and its hydrology and hydrogeology is a common feature of basins in the central and southern Italian Apennines chain. However, our study is not limited to the discharge simulation but is focused on the closure of the whole water budget in this complex systems.

2 Study Area and datasets

2.1 Study area

Nera is the largest tributary of the Tiber and its sources are in the Mts. Sibillini in central Italy. It is is 116-kilometers long and flows almost entirely in a deep valley called Valnerina, through limestone formations that constitute huge aquifers feeding

https://doi.org/10.5194/egusphere-2022-340
Preprint. Discussion started: 12 July 2022

the river. The landscape is mainly hilly and mountainous and is almost totally covered by forests with pastures areas at higher elevations (from 1200 to 2200 a.s.l). The Upper Nera basin at Visso river station (our study area) covers an area of around 110 km^2 and the elevation ranges between 570 and 2200 m a.s.l. with a mean basin slope of 25 percent. The basin is characterized by a Mediterranean climate, with precipitation occurring mostly in the autumn–spring period when floods generally occur.

Nera discharge is affected by a set of permanent linear springs fed by large limestone aquifers already studied in Boni et al. (1986) that give rise to several episodes of surface-groundwater water interactions. Nanni et al. (2020) and Mastrorillo et al. (2019) showed how these aquifers extend beyond the limits of the river basin in the wide and complex hydrogeological boundary of the Sibillini Mountains. Mastrorillo et al. (2019) estimated that the total contributing area of the carbonate fractured system outside the geomorphological boundaries of the basin (our study area) is around 97 km^2. Fronzi et al. (2021) applied several tracer tests showing that the river (from southern east of the basin) is fed by the carbonate aquifers with an area almost 4 times larger than the one enclosed by the river station of Castelsantangelo located at the upstream of Visso (Fig. 1(a)). Similar findings were found for the Ussita river – the main tributary of Nera at Visso – characterized by a real contributing area almost double its geomorfological boundaries (Mastrorillo et al., 2019).

2.2 Terrain data and ground Meteorological network

The terrain data for the geomorphological analysis of the basin were provided by Marche Region. The Horton Machine Toolbox (Abera et al. (2017)), was used to define the basin the geomorphological boundaries shown in (Fig. 1(a)), and the basin was further subdivided into 47 Hydrologic Response Units (HRUs) (Fig. 1(b)).

The meteorological network of the area currently consists of 32 precipitation gauges, 21 thermometers, and 3 hydrometric stations distributed throughout the territory. Metereological and hydrometric datasets provided by regional authority (Marche Region) are freely available, but they were additionally provided in the supplemental material for the readers' convenience. The monitoring network provides 15-minute data for which a quality-check to remove anomalous values and re-sampling to hourly resolution were performed. Streamflow data were calculated by the transformation of water levels measured at hydrometric stations via rating curves updated every 2 years. The recorded streamflow at three main hydrometric stations specified in Fig. 2 have been applied for developing the models. The stations are Visso and Castelsantangelo (CSA) on the Nera River and Madonna dell'Uccelletto (MU) on the Ussita River.

Visso station is the one located lowermost of the case study. Its data, covering the period 2007–2021, were used for the hydrological analysis. CSA station, with available data in the period of 2009-2017, is located upstream of the basin and is affected by a significant proportion of groundwater discharge coming from the external area (Fronzi et al., 2021) which will be addressed comprehensively in the next sections. Hereafter, the discharges related to the period of 2016-2017 affected by the seismic sequences have been excluded from the analyses since the earthquake altered the groundwater contribution of the fractured system determining an abrupt and sustained change in the river and spring discharges in several parts of the basin (Di Matteo et al., 2020, 2021). My hydrometric station on the Ussita River is characterized by about 4.5 years of hourly data starting from 2017.

https://doi.org/10.5194/egusphere-2022-340
Preprint. Discussion started: 12 July 2022

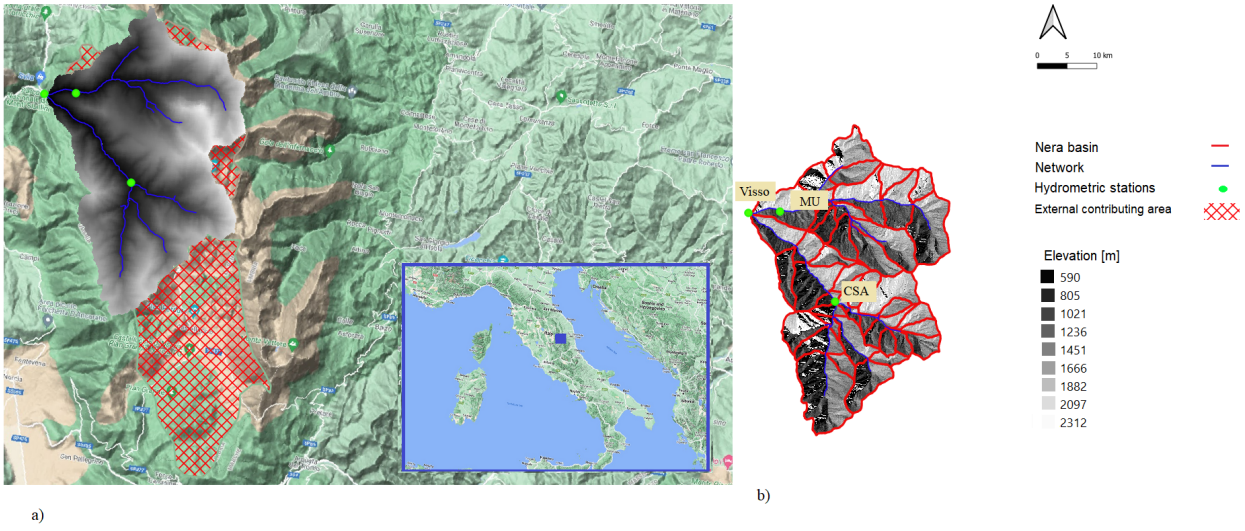

Figure 1. (a) The study area with the DEM of the basin, additional external area and the hydrometric stations locations in the network. (reworked and modified from from © OpenStreetMap contributors 2022. Distributed under the Open Data Commons Open Database License (ODbL) v1.0.) (b) Delineation of the HRUs in the hydrological basin based on the generic method (shape and morphology of the basin).

Table 1. Characteristics of the Visso, Castelsantangelo and Ussita hydrometric stations.

Station	**River**	**Geom. basin area**	**External contributing area**	**Total area**	**Record**
-	-	[km^2]	[km^2]	[km^2]	[yr]
Castelsangelo (CSA)	Nera	17	70	87	2009-2017
Visso	Nera	110	110	220	2007-
Madonna dell'Uccelletto (MU)	Ussita	45	40	85	2017-

Table 1 summarises the total contributing area of the three hydrometric stations (based on the literature), which includes the one fed by external groundwater contribution and the basin area derived from the terrain analysis can be estimated to be equal to 220 km^2, 85 and 87 km^2 for Visso, MU and, CSA, respectively (see Fig. 1(a) and Table 1).

2.3 Remote sensing data

Remote sensing data of evapotranspiration (ET) and the snow cover were also used to complement the validation. In particular, we used MODIS actual ET (Mu et al. (2013)) and the Sentinel-1 snow depth Lievens et al. (2019)). The global MODIS ET data set MOD16A2 and MYD16A2 provides evaporation from wet and moist soil, evaporation from rain water intercepted by the

https://doi.org/10.5194/egusphere-2022-340
Preprint. Discussion started: 12 July 2022

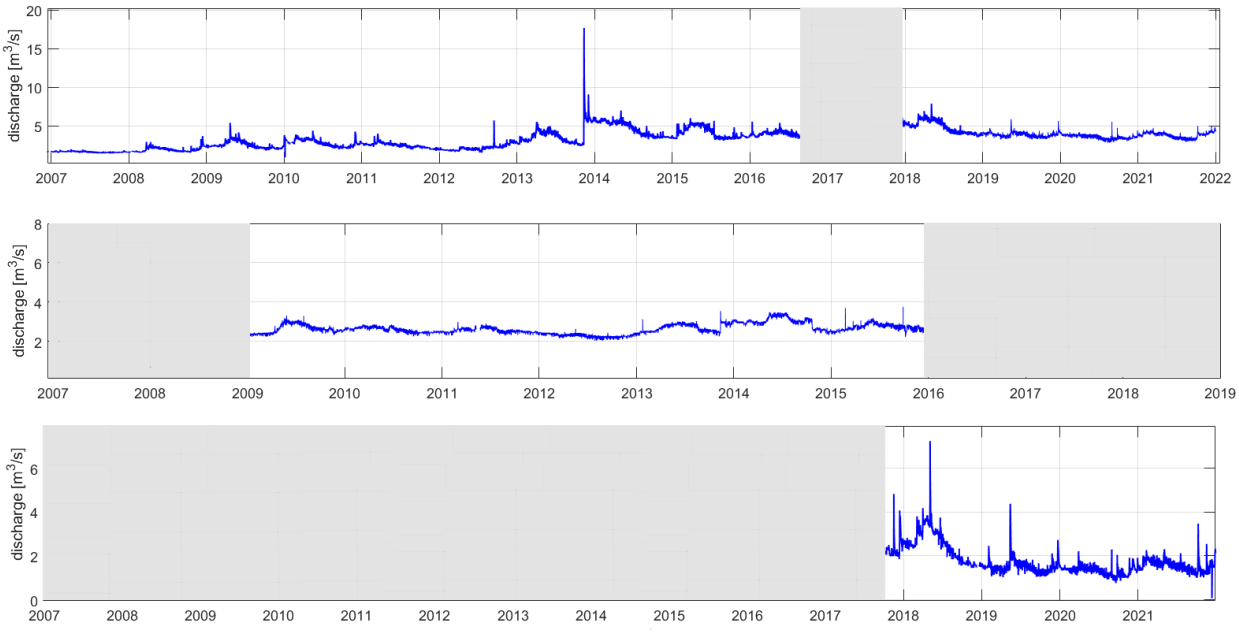

Figure 2. The discharge time series at the outlet of (a) Visso, (b) CSA and (c) Ussita stations. The discharge values are not available for the gray color periods and have been eliminated from the hydrological analysis. All the time series are hourly.

canopy before it reaches the ground and the transpiration through stomata on plant leaves and stems with 500m spatial and 8-day temporal resolutions (Mu et al. (2013)). The data set is downloadable from (http://files.ntsg.umt.edu/data/NTSG_Products/MOD16/).

The Sentinel-1 snow depth retrieval algorithm is based on an empirical change detection method applied to the measurements of the cross-polarization ratio ($\sigma^0_{vh}/\sigma^0_{vv}$; in dB). For more details about Sentinel-1 snow product, the reader are referred to the main reference (Lievens et al. (2019)). The Sentinel-1 snow depth retrievals are available online at https://ees.kuleuven.be/project/c-snow.

3 Hydrological characterization of the basin

Prior to determining the contribution of groundwater to river discharge in relation to the other components of the water balance, we analyzed the precipitation and river discharge time series by focussing on the area derived from the terrain analysis (i.e., external area contribution excluded, Table 1). The comparison of the cumulative precipitation against cumulative river discharge observed at the CSA outlet (Fig. 3(a1)) provides a proper insight into the hydrological behavior of the external part of the basins owing that the runoff is much larger than the precipitation. Fig. 3(a2) shows the runoff coefficient of the basin at CSA, computed through dividing the discharge of CSA by the precipitation time series, ranges between 4 and 5. This means that assuming as null hypothesis that the mean precipitation is constant in the red shaded area of Fig. 1, the basin contributing to the CSA outlet is at least 4 or 5 times larger than the extension of the basin delineated by terrain analysis in line with Fronzi et al.

https://doi.org/10.5194/egusphere-2022-340
Preprint. Discussion started: 12 July 2022

(2021). Fig. 3(c1) and (c2) also show evidences of external groundwater contribution by the carbonate aquifers in the Ussita river determining runoff coefficient larger than one. The relative contribution of external groundwater to the river discharge tends to reduces by moving downstream in Visso as manifested to the smaller runoff coefficient observed here (Fig. 3(b1) and (b2)). Note that panels in Fig. 3(a1, b1 and c1) are obtained with the closest rain gauge stations to the river stations, the remaining plots related to the other rain gauge stations collocated inside and outside the analysed basins are available in the Supplementary material (Fig. 1S & 2S). Similar conclusion can be drawn for MU.

Once verified that the contribution to the basin is much larger than the one provided by the terrain analysis it is necessary to figure out the time delay between the precipitation input and groundwater contribution in the basin. The approach suggested by Giani et al. (2021) is a potential way to do that. In particular, it provides a way for characterizing the time scale of the transformation from a noisy precipitation input to a smoother streamflow output at the outlet. The scope of this approach for the external area is to determine the time lag at which the precipitation and runoff time series are non-linearly correlated, despite the time series have different frequency spectra. In Fig. 4, we applied the method at the CSA and MU and the precipitation over the basin to understand the time lag at which these two variables are most strongly correlated. Fig. 4(a) displays that $\sim$ 30-day (700 hours) is the time window at which the precipitation and discharge of CSA are most correlated in line with the results of Nanni et al. (2020) who showed that the mean tracer transit time (days) is around 26(+/-3) days for CSA. We attributed the first time window (3 days/70 hours) with a high correlation to the subsurface runoff response and the second to the groundwater contribution to the total runoff. The latter is in line with Nanni et al. (2020) who highlighted the presence of a basal aquifer feeding the springs in the wide and complex hydrogeological boundary of the Sibillini Mountains specifically on the Upper Nera basin. Tracer tests conducted later by Fronzi et al. (2021) demonstrated that the springs emerge along Nera River Valley and directly feed the river, as well as some linear springs emerging a few kilometres downstream,. Fronzi et al. (2021) also showed that the CSA river is fed by the aquifer with a recharging area almost 4 times larger than CSA (Fig. 1). For MU, Fig. 4(b) demonstrates that 17-day (400 hours) and 167-days (4000 hours) are the window lengths in which the discharge and the precipitation are most correlated. Evidences of a delayed external groundwater contribution in the Ussita River discharge are also present in Mastrorillo et al. (2019) who showed that a fraction of the total external area contribution of the Nera River feeds Ussita River basin before MU (see Table 1).

Another aspect that the data reveal is that in some years, 2010 to 2012, the discharge does not increase from CSA to Visso. In the other years of which we have records, discharge is increasing approximately at the same rate for MU-Visso and for CSA-Visso, less than linearly with the upstream area. The anomalous years 2010-2012, have been characterized by the extremely dry climate.

4 Methods for modelling basins with external groundwater contribution

Generally, the shape and topology of the superficial basin give a guide to separate the pathways of water and to obtain, by interpolation over the basin area, the precipitations volumes for each sub-basin. This general approach is evidently not

https://doi.org/10.5194/egusphere-2022-340
Preprint. Discussion started: 12 July 2022

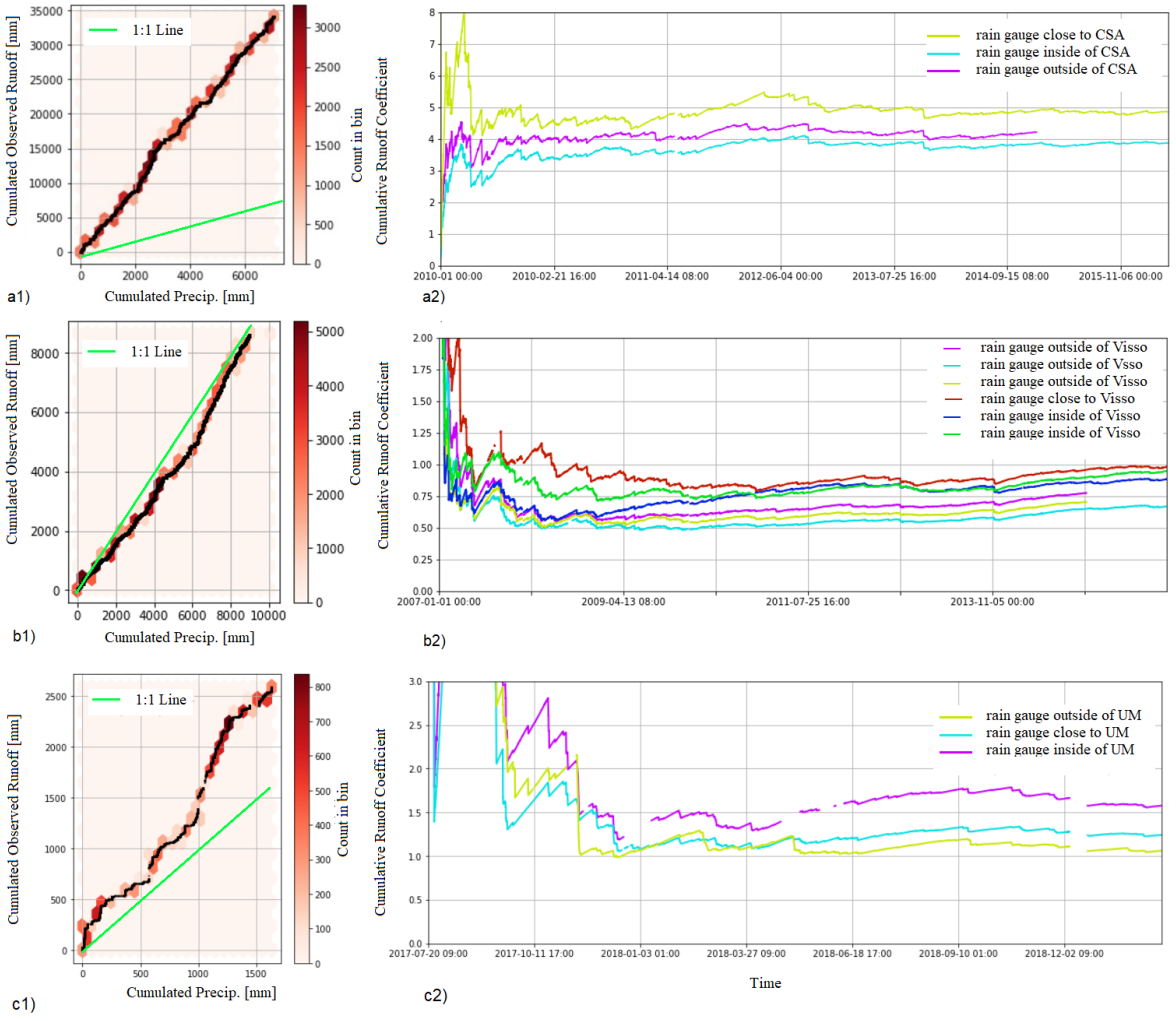

Figure 3. (a1) Cumulative CSA observed discharge against cumulative precipitation recorded at the closest station to CSA, (a2) Coefficient time series computed through dividing the discharge of CSA by the precipitation time series recorded at different stations. (b1) Cumulative Visso observed discharge against cumulative precipitation related to a station close to Visso, (b2) Coefficient time series computed through dividing the discharge of Visso by the precipitation observed at several stations. (c1) Cumulative Ussita observed discharge against cumulative precipitation related to a station close to Ussita, (c2) Coefficient time series computed through dividing the discharge of Ussita by the precipitation observed at several stations. The 1:1 line is shown in green. For CSA and Ussita, the runoff coefficient is around 4 and 1.5, respectively, and this values is still high at the outlet of the basin (Visso)

https://doi.org/10.5194/egusphere-2022-340
Preprint. Discussion started: 12 July 2022

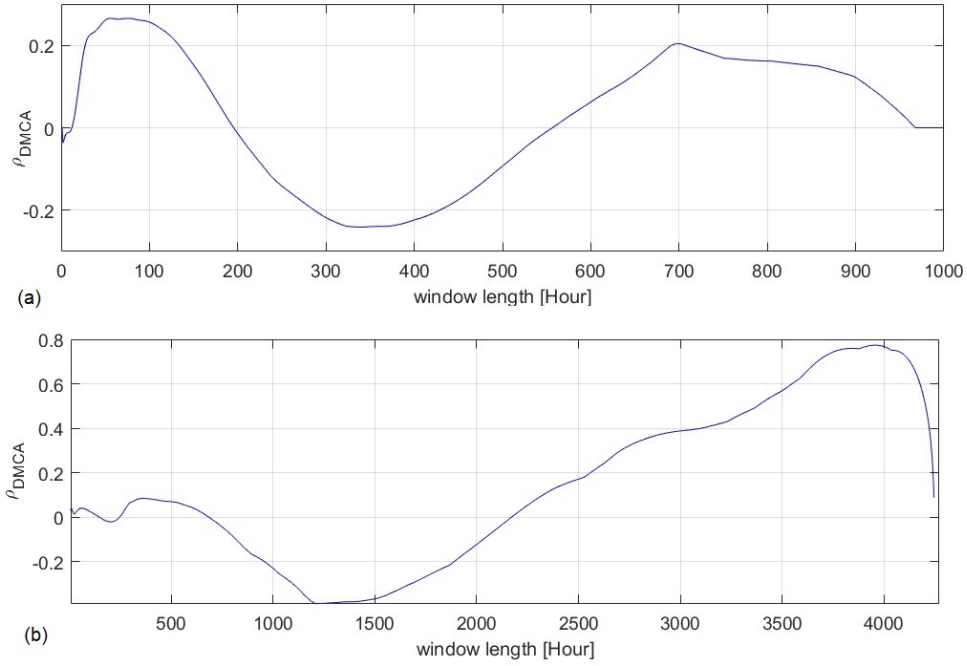

Figure 4. The correlation of noisy precipitation time series and the smoother (a) CSA and (b) Ussita discharge with different window length. For CSA, 3-day (around 70 hours) and 30-day (700 hours) are the window lengths in which the precipitation and runoff are more linked. The first one should be related to the basin response and the latter is related to the water recharge coming from karst and fissured rocks. The low correlation values should be since of the smooth CSA discharge compared to the precipitation frequency. For Ussita, 17-day (around 400 hours) and 167-day (around 4000 hours) are the window lengths that the precipitation and discharge are correlated. The high correlation of the 167-day delayed precipitation with the discharge would be associated with the slow response of the aquifer.

applicable in the case of the Upper Nera basin as also evidenced by the values of the runoff coefficients in the last section. However, according to the field survey and measurements conducted by Mastrorillo et al. (2009) and Nanni et al. (2020), the extension of the contributing basin area has been determined but the groundwater pathways are still unknown.

4.1 Model structure

For optimal modeling of karst and fissured systems, the basin area can be split into two main parts: surface basin (SC) and the "external aquifer" basin (AC). As it has been already mentioned, the SC has been partitioned into the 47 HRUs, while the ACs were considered as unique sub-basins where the water flux flows into the SC from the head of the CSA and MU.

The snow contribution was taken into account for both SC and AC as shown by the Extended Petri Net (EPN) in Fig. 5. In particular, the latter shows that according to the air temperature, precipitation flux is partitioned into snowfall and rainfall (Formetta et al. (2014)). Then, snow can eventually melt and increase the liquid water and thereafter it can either refreeze or flow while being transferred to the vegetation reservoir. Afterward, the input flux into the canopy reservoir either evaporates

https://doi.org/10.5194/egusphere-2022-340
Preprint. Discussion started: 12 July 2022

Symbol	Name	Unit
Snow Reservoirs		
M	Melted Water	[L T^{-1}]
M^d	Runoff Melted water	[L T$_{-1}$]
P	Precipitation	[L T$_{-1}$]
P_r	Liquid Precipitation	[L T$_{-1}$]
P_s	Snowfall	[L T$_{-1}$]
R	Refrozen Water Rate	[L T$_{-1}$]
SWE	Snow Water Equivalent	[L]
T	Temperature	[K]
W_s	Liquid Water in snow	[L]
Canopy Reservoirs		
ETc	Evaporation from wetted canopy	[L T^{-1}]
Md	Runoff Melted water	[L T^{-1}]
Tr	Throughfall	[L T^{-1}]
U_1	Fast Runoff	[L T^{-1}]
U_2	Slow Runoff	[L T^{-1}]
Runoff Reservoirs in non-karst area		
ET_{RZ}	Evapotranspiration	[L T^{-1}]
Q_R	Surface Water Runoff	[L T^{-1}]
Q_{WG}	Groundwater contribution to the surface runoff	[L T^{-1}]
R_E	Recharge	[L T^{-1}]
S_R	Surface Water	[L]
S_{RZ}	Root Zone Storage	[L]
S_{WG}	Groundwater	[L]
T_r	Throughfall	[L T^{-1}]
U_1	Fast Runoff	[L T^{-1}]
U_2	Slow Runoff	[L T^{-1}]
Runoff Reservoir in karst area		
k	Mean residence time	[T]
Q_{low}	Discharge out of the karst area	[L T^{-1}]
S_{low}	Storage in karst area	[L]

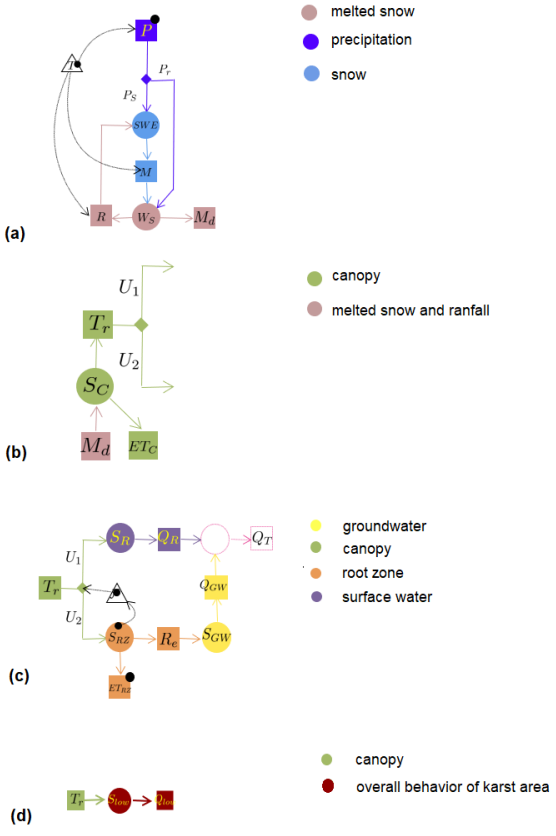

Figure 5. The expressions and Extended Petri Net (EPN) of different components associated to snow (a), canopy (b), runoff (c) and external groundwater runoff (d). For more details about the components of GEOframe-Newage, the readers could refer to Formetta et al. (2014) and Bancheri et al. (2019).

from the canopy or through-falls to the soil (Fig. 5(b)). The part that falls in the soil is partitioned into the three reservoirs presented in Fig. 5(c). For more details on the functionality of the reservoirs, the readers could refer to the main references (Formetta et al. (2014) and Bancheri et al. (2019)). Besides, the Prospero model (Bottazzi et al. (2021)) capable of computing actual evapotranspiration (ET) using a multi-layer canopy model, solving the energy balance both for the sunlight and shadow vegetation, extending the recently developed Schymanski and Or method Schymanski and Or (2017) to canopy level has been applied in this study.

The idea behind creating a specific reservoirs arrangement for the AC is that the destiny of water in the soil is different in the SC and AC areas. Therefore, a different arrangement of reservoirs has been inserted for CSA and MU (see Fig. 5(d)) The

https://doi.org/10.5194/egusphere-2022-340
Preprint. Discussion started: 12 July 2022

AC water flowing into the CSA is conceptualized with a unique reservoir whose travel time parameter is set equal to 30 days while for MU Ussita is modelled with two reservoirs whose the travel times are 17 and 167 days, respectively.

4.2 Experiment setup, calibration, validation and metrics

The model was calibrated with hourly river discharge observed at the hydrometric stations of CSA, MU and, Visso and cross-compared with remotely sensed products of evaporation and snow depth as well as validated with river discharge observations. The comparison with remote sensing observations provides insights into the model's robustness in reproducing spatial patterns of ET and Snow Water Equivalent (SWE) across the study area.

The model was span up at CSA sub-basin in the period Jan 2005- Dec 2009 while Jan 2010 to Dec 2015 period was used for the calibration of the model. For Visso also the warm-up period involved the first 4 years (Jan 2005- Dec 2008) while the following years (Jan 2009 to Feb 2019) were used for the calibration process. Finally, the period of Sep 2017- Dec 2018 was applied for the calibration of model parameters over Ussita. The model is validated based only on Visso and MU stationsduring Jan 2019- Dec 2021 because CSA was not available in this period. Note that, herein the warm-up period was chosen based on the features of the sub-basins.

Based on the results of a sensitivity analysis (not shown), 18 parameters were chosen for the calibration process whose values are reported in Table 3. The model calibration process was performed based on LUCA (Hay et al. (2006)) using the available observed discharge at the mentioned stations. The calibration algorithm was used to maximize the Kling-Gupta Efficiency (KGE) (Gupta et al. (2009)) value between the observed and simulated discharge time series.

Different scores and hydrological signatures (Addor et al. (2017)) were used to evaluate the model robustness (Table 2) including mean daily discharge, high flow, low flow, flow duration curve slope, and low flow duration frequency. In particular, high-flow and low-flow represent the 95^{th} and 5^{th} percentile of the discharge, respectively. The low flow duration frequency originally introduces the frequency of the days with discharge 0.2 times lower than the mean discharge value. Herein, since the Nera River streamflow does not change in a wide range, this signature is considered as the frequency of the days with discharges lower than the average of river flow (and thus not 20 percent of the average discharge). Additionally, for further understanding the discharge behavior, we proposed a new approach for evaluating the model based on an empirical probability. This score is based on the density of the observed discharge conditional on the modeled discharge: $p_e(Q_{obs}|Q_{sim})$, where p_e is the empirical probability, Q_{obs} is the observed discharge and Q_{sim} is the simulated discharge. Figure 6 (a), top left, further commented below, shows these empirical (and therefore discrete) probability density function, with varying Q_{sim}. The method provides a criterion to show how the model statistically performs concerning the historically observed discharge which is optimal if the simulated values are located close to the mode, Coccia and Todini (2011), Barbetta et al. (2016) and Massari et al. (2019). The difference of the discharge value corresponding to the maximum conditional probability and the simulated discharge is the representative of prediction error for Q_{sim}.

https://doi.org/10.5194/egusphere-2022-340
Preprint. Discussion started: 12 July 2022

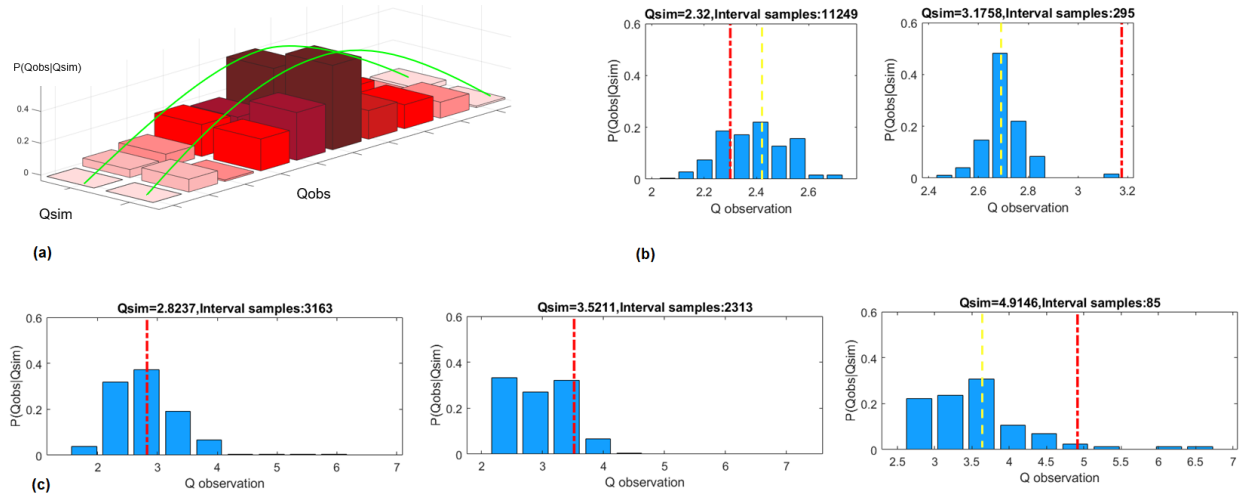

Figure 6. (a) Scheme of the proposed method for computing empirical error as the model score. (b) The examples of computing the proposed score for the simulated discharge Q=2.32 and 3.17 m^3/s in CSA basin and (c) the simulated discharge Q=2.82, 3.52 and 4.91 m^3/s in Ussita basin. In all the plots, the difference of discharge corresponding to the highest probability (yellow dashed line) and the simulated discharge (red dashed line) is equal to the bias of the model.

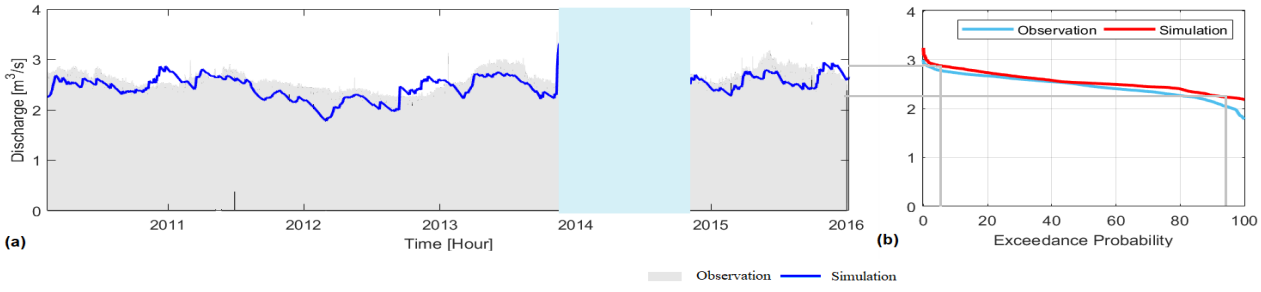

Figure 7. (a) Simulated discharge at the outlet of CSA during calibration period. The part of discharge with low quality has been ignored from the analysis (blue shade). (b) The flow duration curve of CSA discharge. The 95 th and 5th percentile flow are closed values, since the discharge is smooth in this area.

5 Results and discussion from calibration

In this section, we investigated the ability of the GEOframe-Newage system components in reproducing the river discharge and the related internal ET and SWE of the Upper Nera River basin.

https://doi.org/10.5194/egusphere-2022-340
Preprint. Discussion started: 12 July 2022

Table 2. Different applied signature to evaluate the performance of the model

Type of Scores	Name	Description
General Scores	KGE (Gupta et al., 2009)	$KGE = 1 - \sqrt{(r-1)^2 + (\alpha-1)^2 + (\beta-1)^2}$
	Correlation Coefficient	$R = \frac{\sum_{i=1}^{N}(S_i - \bar{M}_i)^2}{\sum_{i=1}^{N}(M_i - \bar{M}_i)^2}$
High Flow	95^{th} percentile of streamflow	95% flow quantile (high flow)(mm yr^{-1})
Low Flow	5^{th} percentile of streamflow	5% flow quantile (lowflow) (mm yr^{-1})
LFD Frequency	Frequency of low flow days	
	(Westerberg and McMillan, 2015)	day yr^{-1}
Flow Duration Slope	Slope of flow duration	
	(Sawicz et al., 2011)	$SFD = \frac{ln(Q_{33\%}) - ln(Q_{66\%})}{0.66 - 0.33}$
Mean Daily Discharge	-	mm day^{-1}

5.1 Model suitability to simulate river discharge

Fig. 7(a) shows the simulated hourly discharge at the outlet of CSA by considering the external reservoir in the model. The obtained KGE (see Table 2 for its definition) and R^2 are equal to 0.61 and 0.65, respectively. Since the discharge flowing from the external area is not calibrated based on the relevant observed values and considering the willing to maintain the model structure as simple as possible, these values are more than acceptable. According to the Fig. 7(b) and the value of CSA flow duration curve slope in Table 3, it seems that there is no considerable discrepancy between the high (95 th percentile) and low (5 th percentile) flow in CSA.

Regarding LFD frequency signature in Table 3, during most of the days in the year, the discharge values are lower than the average river flow showing that the distribution of discharges is left-skewed. All the signatures in the Table are well reproduced, even if the calibration was not targeted on them. High flow statistics show a discrepancy of -5% and Low flow statistics bias is greater, since the difference is around -10%. The duration curve of the simulated behavior is a 30% steeper meaning that the actual discharges are, on average, more varying than the simulated ones, even if the latter, have higher extremes. The discrepancy between simulated and observed mean discharge is, however, limited to less of 3%, which can arguably be considered below the heuristically expected uncertainty of the forecast. It should be noted that due to different period of calibration in the three hydrometric stations, the average daily discharges are not comparable with each other.

Fig. 8(a) shows the simulated discharge at the outlet of the basin (Visso station) characterized by R^2 and KGE equal to 0.84 and 0.80 for the calibration period and 0.64 and 0.68 for the validation period (splitted by the green line), respectively which is a sensible improvement with respect to CSA. Similar to CSA, the frequency of low flow score, which is 205 days

https://doi.org/10.5194/egusphere-2022-340
Preprint. Discussion started: 12 July 2022

Table 3. Different Signatures of simulated and observed flow during calibration period at CSA, Visso and MU hydrometric station. Note that the calibration period is different in the three hydrometric stations and the average daily discharges are not comparable with each other.

Data	High Flow	Low Flow	LFD Frequency	Flow Duration Slope	Mean Daily Discharge
CSA basin					
Observation	2.9	2.23	208	0.19	2.55
Simulation	2.78	2.03	180	0.25	2.48
Visso basin					
Observation	5.6	1.66	205	1.35	3.2
Simulation	5.19	1.90	211	1.03	3.15
Ussita basin					
Observation	3.6	1.59	198	0.85	2.46
Simulation	3.5	1.82	208	1.04	2.52

for the observed discharges, demonstrating that the low flows are dominating in the river also at the outlet of Visso (except for the Nov-2013 event). However, at Visso, the model estimates more days of low flow (211) than observed, while at CSA was the contrary happens. Considering Table 3, the comparison of the slope of flow duration curve for Visso and CSA is a good evidence of lower oscillation of flow in CSA, since the curve is more than five time steeper. Fig. 8 also shows the empirical error in each time step, based on the method mentioned in section 4.2 in which the simulated discharges being close to the darker colors shows the robust performance of the model in describing the system.

Fig. 6(b) & (c) represent a complementary view to the one offered by Fig. 8. It is apparent that the model is very good at reproducing the lowest discharges (which are predominantly in number as annotated in Fig. 1S & 2S), while it is biased for the largest discharges and simulates discharge values in a larger range of variability. According to the statistical analysis carried out in Fig. 6(b), the model has a bias around 0.07 and 0.47 m^3/s for modeling the CSA discharges equal to 2.32 and 3.17 m^3/s, respectively.

Fig. 9(b) displays the simulated discharge at MU with R^2 and KGE obtained equal to 0.61 and 0.71 during calibration period, and 0.50 and 0.48 during validation period, respectively. Table 3 presents different scores related to the signatures which show a relatively good agreement. Although the long-term average value of discharge is almost the same in CSA and Ussita, the difference between low and high flows at MU is higher (Table 3) than those of CSA. This confirms the dissimilar river regime behavior in these two parts of the basin. As well, the flow duration slope showing in Table 3, declares the higher variation of discharge at MU than CSA. Additionally, based on Fig. 6(c), the model has an empirical error around 1.4 m^3/s for modeling

https://doi.org/10.5194/egusphere-2022-340
Preprint. Discussion started: 12 July 2022

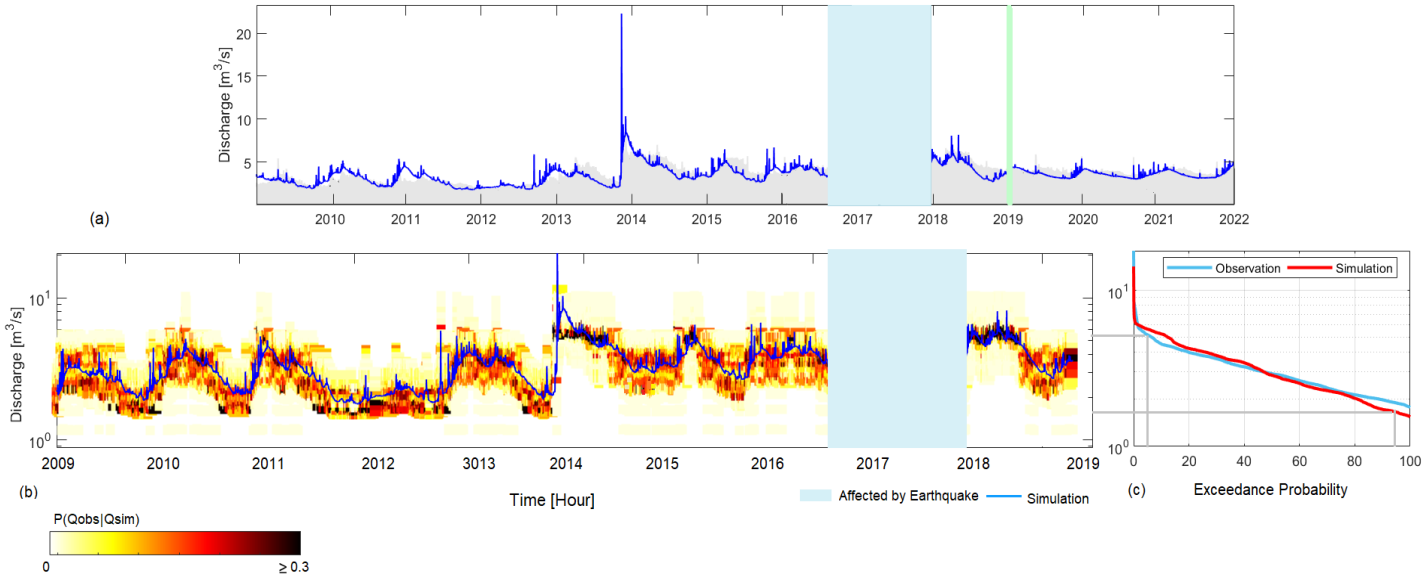

Figure 8. (a) Simulated discharge at the outlet of Visso during calibration (2009-2018) and validation periods (2019-2021) splitted by green line. The discharge affected by the earthquake has been ignored from the analysis (blue shade). (b) The shadow color shows the the conditional probability p(Qobs|Qsim). The more the simulation is closer to the darker color, the more robust model performance is excepted. (c) The flow duration curve of Visso discharge for the calibration period. The 95 th and 5th percentile flow are determined in the figure.

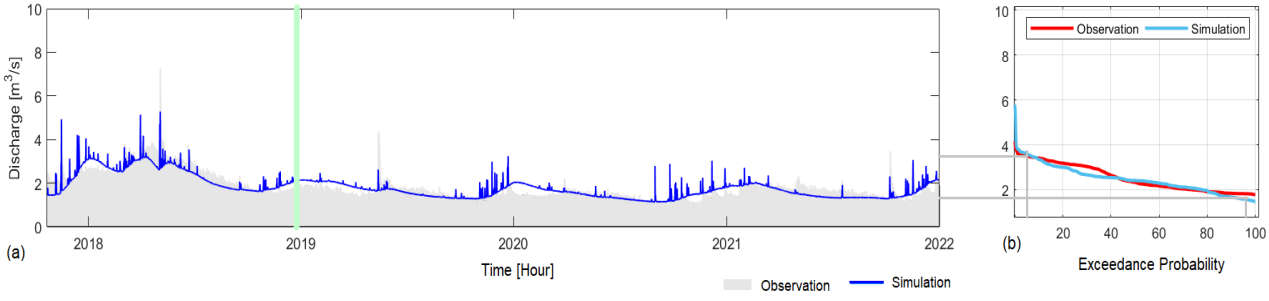

Figure 9. (a) Simulated discharge at the outlet of Ussita for the calibration (mid of 2017-2019) and the validation (2019-2021) periods splitted by the green line. (b) The flow duration curve of Ussita discharge for the calibration period. The 95 th and 5th percentile flow are determined in the figure.

Ussita discharges around 5 m^3/s and the model performs almost correctly for estimating the discharges around 2.8 and 3.5 m^3/s.

https://doi.org/10.5194/egusphere-2022-340
Preprint. Discussion started: 12 July 2022

5.2 Evapotranspiration (ET)

A comparison of GEOframe-Prospero ET and the remotely sensed actual ET from MODIS product (Mu et al. (2013)) (which is based on Penman-Monteith relation and various measured optical quantities) is shown in Fig. 10(a1-a4). The figure shows that the simulated and remotely sensed actual ET for two CSA sub-basins characterized by different elevations and located at 696 and 1615 meters above sea level, respectively. The two ET time series show good correlation with correlation coefficients equal to 0.86 and 0.78, respectively. Furthermore, the figure displays that MODIS hindcasts much higher ET values than Prospero (i.e., is less sensitive to stresses than Prospero) and the total amount of difference has been calculated to be 180 mm per year on average.

Likewise, the comparison of GEOframe-Prospero and MODIS actual ET, for two sub-basins located at 778 and 824 m.a.s.l, has been shown in Fig. 10(b1-b4), with the correlation values equal to 0.76 and 0.77, respectively. In terms of bias, being the study area relatively small and the MODIS ET partially based on large scale forcing, some positive systematic differences are somehow expected because the forcing used in MODIS embraces a much larger area at lower elevations than the surrounding the basin thus potentially determining an overestimation of the evaporative demand.

5.3 Snow

The current version of GEOframe snow component provides the Snow Water Equivalent (SWE) and not snow depth, a comparison between the model results and the Sentinel-1 EO product was done only in terms of correlation. In particular, in each time step, the spatial correlation between SWE of the model and snow depth of Sentinel-1 was considered and calculated with N values, where N is the number of HRUs. Fig. 11(a) and the associated box plot show the spatial correlation of Sentinel-1/GEOframe snow cover over time for CSA. To avoid uncertainties related to the snow compaction (SWE vs snow depth), only the time span of Dec-Mar has been considered in the analysis which correspond to the snow accumulation period. According to the figure, the 75th and 25th percentile of correlation are in the range of 0.79 and 0.5 for the CSA basin. A relatively good agreement of Sentinel-1 and in-situ snow depth over CSA (Fig. 3S), could conclude the relatively good performance of the model in snow simulation.

Fig. 11(b) presents the spatial correlation between Sentinel-1 snow depth and GEOframe SWE for the HRUs of the Nera River basin in the period of December-March at Visso. Despite the fact that the two quantities are not always theoretically comparable (this is the reason why we only selected the December-March period), there is a relatively good agreement – between the variables– which tends to reduce at the end of the snow season as expected. This agreement is relatively lower for the Ussita sub-basin as it can be clearly seen in the same figure (Panel c) but we do not have sufficient elements to explain the reason.

https://doi.org/10.5194/egusphere-2022-340
Preprint. Discussion started: 12 July 2022

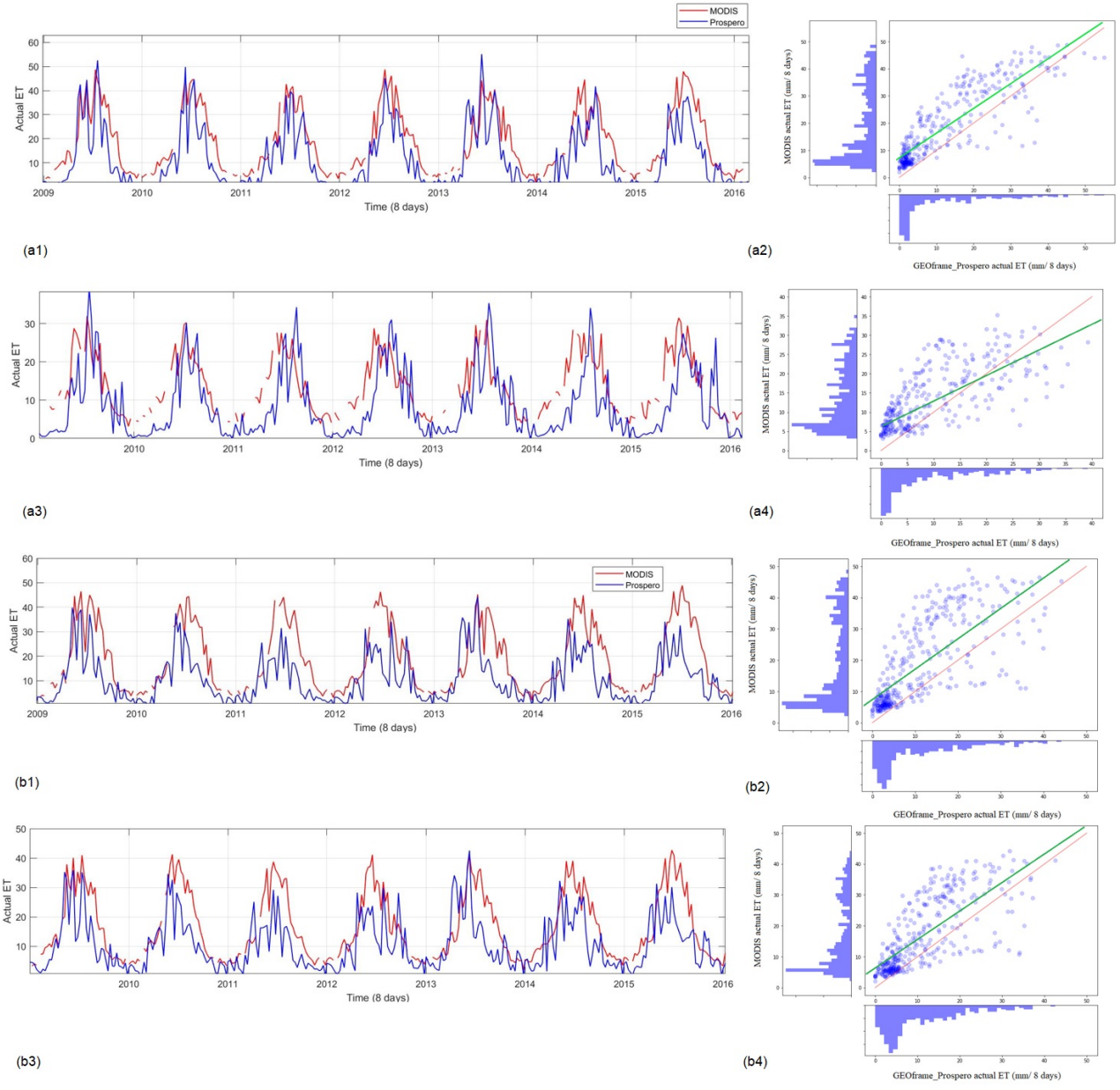

Figure 10. The MODIS and GEOframe-Prospero actual evapotranspiration as long as the associated scatter plots for the two CSA sub-basins located at 696 m.a.s.l (a1 and a2) and 1615 m.a.s.l (a3 and a4). Green and red lines show the regression and 1:1 lines in the scatter plots, respectively. The same comparison of actual evapotranspiration and the corresponding scatter plots for the two Nera sub-basins located at 778 m.a.s.l (b1 and b2) and 827 m.a.s.l (b3 and b4). The Green and red lines show the regression and 1:1 lines in the scatter plots, respectively. In higher elevation, larger discrepancy of the actual ET is observed.

https://doi.org/10.5194/egusphere-2022-340
Preprint. Discussion started: 12 July 2022

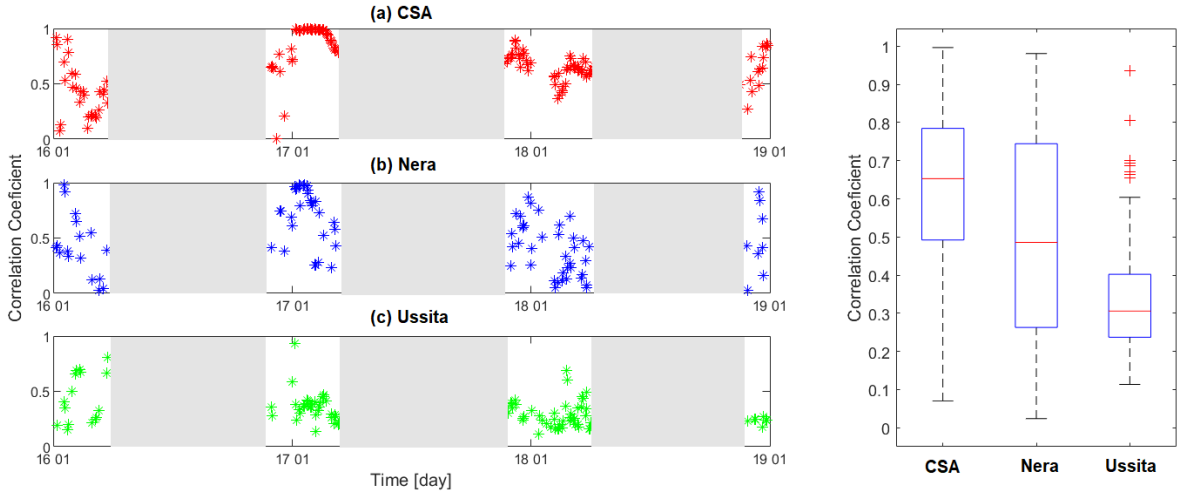

Figure 11. The spatial correlation of Sentinel-1 and GEOframe snow cover over the time and the corresponding box plots for CSA (a), Nera (b) and Ussita (c) basins.

5.4 Water budget calculation and the effect of groundwater discharge on the river regime

In this section, we resolve and discuss the different aspects related to the water budget in the area. For any of the (geomorphologically) delineated subcatchments the budget can be written as:

$$\frac{dS}{dt} = P + Q^{\bullet}_{AC} - ET^{\bullet} - Q^{\bullet} \tag{1}$$

where the $\bullet$ indicates that the quantity was estimated by GEOframe, S is the water storage change in the subcatchment, P the total precipitation, Q_{AC} the additional discharge provided by the karst and fissured rocks, ET the evapotranspiration and Q the discharge at the outlet. Fig. 12 shows the mean annual values of water budget components over CSA from 2009 to 2018. It can be seen that the annual groundwater discharge flowing into the river includes almost 85 percent of discharge drained at CSA hydrometric station. Additionally, after groundwater discharge, ET flux is the most important component of water balance in CSA.

According to Fig. 12, the storage estimated as the residual of the other quantities is almost positive (except 2011 as a result smaller precipitation) and highly inter-annually variable which is confirming the existence of an external resource recharging into the CSA basin.

Fig. 13 displays the mean annual water budget fluxes (2009-2018) over the basin closed at Visso station. According to the figure and in comparison to Fig. 12, the effect of external groundwater contribution in relation to the other components of the water budget is attenuating in the basin (see the bars associated with external groundwater discharge). Similar to the CSA basin, in 2013 we have the maximum annual precipitation over the basin and consequently the maximum increase of external groundwater discharge has been observed in this year. However, the same trend of the annual external groundwater discharge flux at CSA/Visso stations is observed in Fig. 12 and Fig. 13, but the effect of external discharge during the period of 2009-2012

https://doi.org/10.5194/egusphere-2022-340
Preprint. Discussion started: 12 July 2022

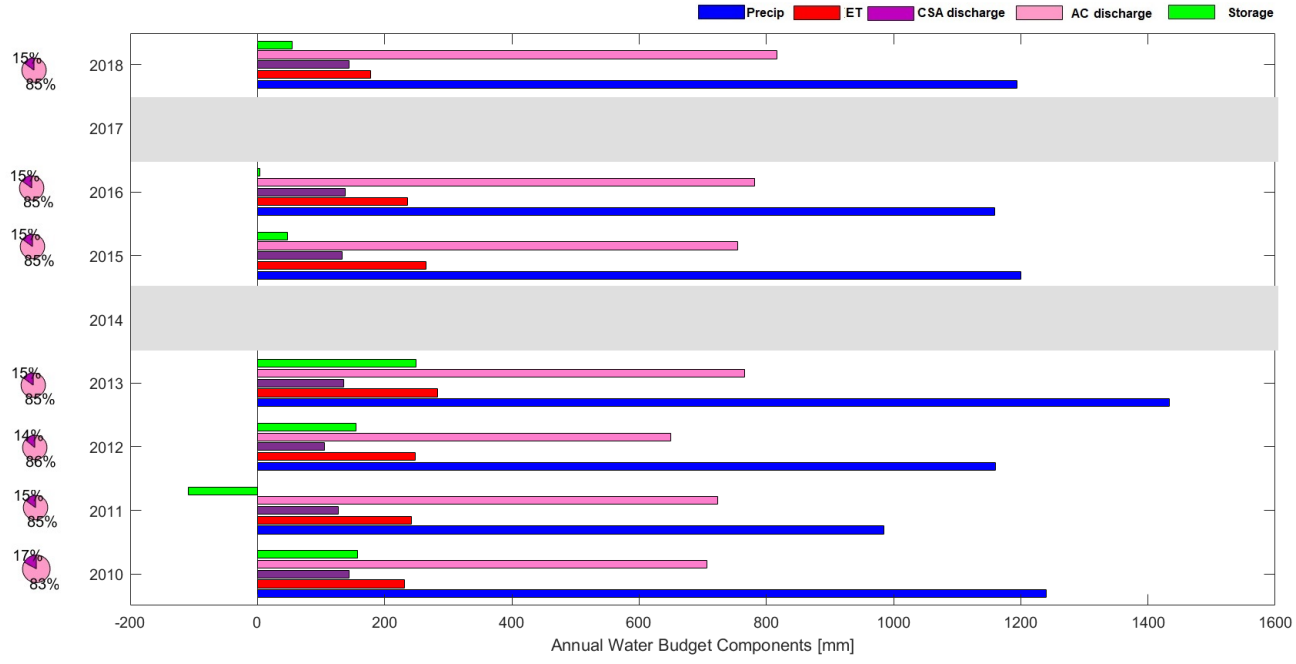

Figure 12. The mean annual water budget components (mm) over the CSA basin from 2010 to 2018. The largest component of water budget in the basin belongs to Q_{AC} which includes 85 percent of CSA river regime. In the next order, ET is the largest component of water cycle in CSA. The residual of water balance equation has been considered as the relative storage of the basin. Where data were not available, due to either instrument malfunctions or earthquake, the analysis is not shown (gray shade). The pie charts show the contribution of external aquifer and and surface runoff in CSA discharge in pink and purple, respectively.

is very low on the Visso river regime. Fig. 12 & 13 also shows that during 2009-2011 discharge values remain almost similar in CSA and Visso (converting the values to $m^3/2$ to make sense). Assuming that ET is not varying too much in the contributing area between Visso and CSA stations, we have to conclude that the excess of discharge has been feeding the aquifer. To confirm this important issue, hydrogeological investigations by (Valigi et al. (2020)) showed that springs recharged by Maiolica and Scaglia formations as the linear springs located between CSA and Visso (exactly where we observe the discharge reduction) showed a great decrease in the discharge while this did not happen on those fed by Calcare Massiccio formation recharged by regional base flow. For example, Pescara spring, in the southern portion of Mt Sibillini on the Maiolica and Scaglia formations, showed a minimum discharge of 50 l/s (vs a minimum discharge in other years at least equal to 250 l/s) and a lack of clear recharge signal (Valigi et al. (2020)). This could explain the behaviour of the discharge in the two years. Evidently, during the drought years, the aquifer was partially depleted at deeper depths. In any case, the excess water, fallen in the area between CSA and Visso has been clearly used for recharging the aquifer, instead than producing runoff.

https://doi.org/10.5194/egusphere-2022-340
Preprint. Discussion started: 12 July 2022

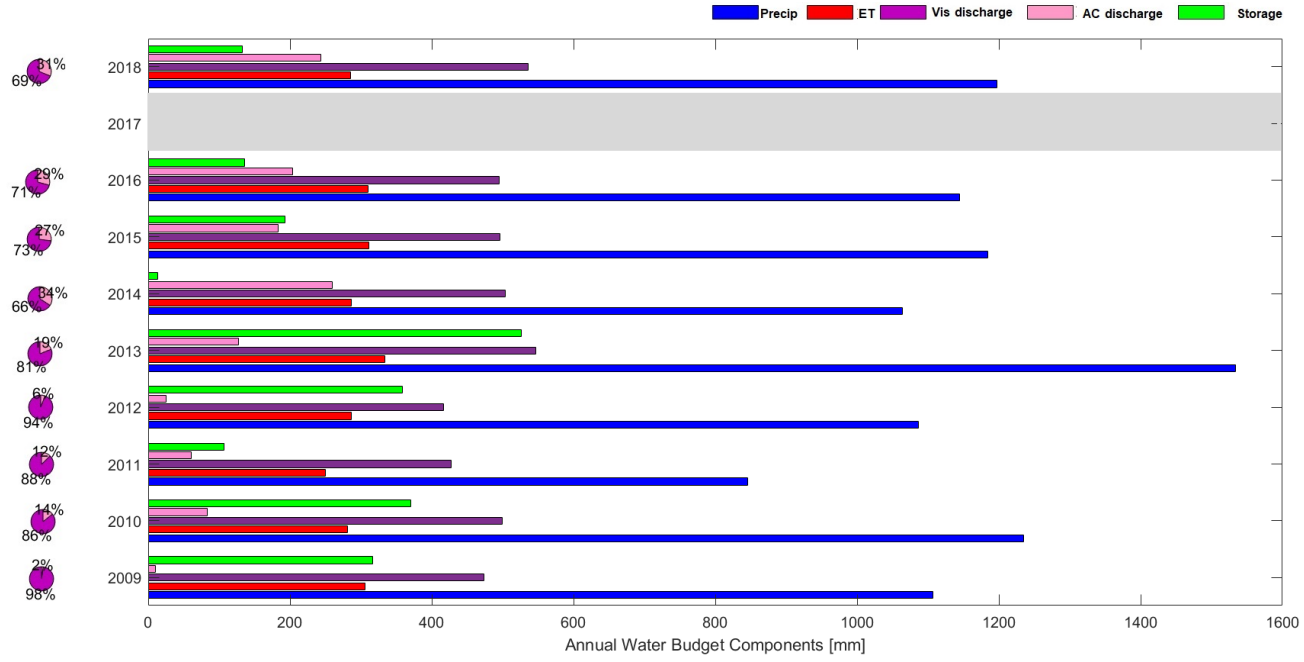

Figure 13. The mean annual water budget components (mm) over the Visso basin from 2009 to 2018. The external groundwater discharge is attenuating through the basin. Visso discharge (without considering karst and fissures flux) is the largest component of water cycle over the basin. The residual of water balance equation has been considered as the relative storage of the basin. In case of unavailability of date, due to either instrument malfunctions or earthquake, the analysis is not shown (gray shade). The pie charts show the contribution of external aquifer and surface runoff in Visso discharge in pink and purple, respectively.

6 Conclusions

Dealing with the Karst and fissured rocks catchments is generally problematic due to the difficulties in determining different recharge areas of aquifers feeding rivers. In other words, the geohydrological basin is often not coincident with the geomorphological one, including extended zones out of the basin itself. In this study:

1. we leveraged the use of hydrogeological surveys and time series analysis to assist the hydrological modelling of the Upper Nera River basin – a complex fissured (and partially karst) rock catchment located in the Apennines chains in central Italy. We showed that the classical approach for delineating river basin is not appropriate and a preliminary check on the water balance closure has to be always carried out if doubts about external groundwater contributions in the river basin exist (see section 3). In particular, we found runoff coefficients in the upper part of the basin to reach values between 4 and 5 (Fig. 3 & 4).

2. we exploited time series analysis to determine the typical response time of the catchments which was found to agree with the estimations given by the field surveys with tracers studies. In particular, the inclusion of additional groundwa-

https://doi.org/10.5194/egusphere-2022-340
Preprint. Discussion started: 12 July 2022

ter reservoirs with a average response time estimated by the rainfall-discharge correlation considerably improved the performances of the modelling solution.

3. we showed therefore that in order to reproduce reasonable river discharge estimates, the hydrological model choice is paramount in the sense that the adopted model must be structurally flexible and easily configurable to be adapted to the experimental evidences. In other words, a model built according to "modelling by components" like Geoframe permits to tailor the model structure to the specific hydrological system straightforwardly. In particular, the basin area was split into two main parts: surface basin (divided in 47 HRUs) and two the karst/fissured rocks basins simulated without any calibration with a simple reservoir model with an avergae response time of 30 days and 170 days for CSA and MU, respectively (Fig. 5). The model, evaluated by different signatures and a proposed empirical probability function, reproduced different water fluxes of the hydrological cycle in the basin relatively well (KGE values equal to 0.61, 0.80, and 0.71 in CSA, Visso, and Ussita sections, respectively, Fig. 7, 8, and 9, Tables 3).

4. we cross-validated evapotranspiration and snow cover with high spatial resolution remote sensing products showing relatively good agreement in terms of dynamic suggesting robust modelling results and no overfitting problems.

5. We found that groundwater discharge flux (partly karst and and mainly from from fissured rocks) has a significant effect on the water budget of the basin, specifically, in the upstream part (CSA). We showed that 85% in proportion to the total discharge at Castelsantangelo station flows from outside of the geomorphological boundary of the basin (Fig. 12 & 13). This influence decreases downstream at the outlet of Visso but it is still present and impact the overall water budget.

This study has clearly presented the limitations associated with a blind, terrain based, identification of the contributing area which can be certainly improved through a combined method involving isotopes and artificial tracers. However the improvement could be achieved paying attention to the rainfall-discharge correlation statistics in a more straightforward way.

Given the complex surface-groundwater interactions and the complex nature of the underground basin, the results found here provided insights about the challenges of modelling river basins with external groundwater contribution. This exercise might be challenging with the classical approach of basin delineation with terrain data, with the use of classical state-of-the-art hydrological models (i.e., flexible and component-based models are needed to model the specific hydrology of the basin) and without a minimum knowledge of the hydrogeology of the area.

Data availability. The input data, simulations, simulated results, the Jupyter notebooks containing the analysis of the data, and the executable project are available on the paper OSF project at: https://osf.io/xtu4g/. The reader can download the OMS3 project, re-execute all the passages and check anything of what has been done in the paper. Everything can be used upon proper citation. Some works are required prior to any simulation with GEOframe. All of this is well documented through slides and videos on the GEOframe blog. The most recent material could be found at: https://geoframe.blogspot.com/2021/12/geoframe-winter-school-2022-gws2022.html. The Sentinel-1 snow depth retrievals are available online at https://ees.kuleuven.be/project/c-snow.

https://doi.org/10.5194/egusphere-2022-340
Preprint. Discussion started: 12 July 2022

Code availability. The source code of the model components used in this paper are available at the GEOframe components Github site: https://github.com/geoframecomponents. The link https://github.com/giuliagiani/Tr_DMCA was used to retrieve the algorithm for the analysis by Giani et al. (2021).

Author contributions. All the Authors revised the paper and agreed on its contents. SA, CM, GF, SB and RR conceived the paper. SA, CM, GF and RR wrote the manuscript draft. GF wrote the Java codes specific to this paper. SA did most of the computations. SA and RR contributed the Python code for the analyses. AlT and DF performed the geological surveys, analyses and catchment identification in the field. SA, SB, SM and AT provided the EO data and did the quality check of the ground based data. CM, GF and RR provided support to the research with their projects.

Competing interests. We declare that no competing interests are present.

Acknowledgements. This paper has been partially supported by MIUR Project (PRIN 2020) "Unravelling interactions between WATER and carbon cycles during drought and their impact on water resources and forest and grassland ecosySTEMs in the Mediterranean climate (WATERSTEM) " (protocol code: 20202WF53Z) and "WAFER" at CNR (Consiglio Nazionale delle Ricerche). The authors would like to also thank the Monti Sibillini National Park, the Marche Region Authority: Ufficio Speciale Ricostruzione Marche and Centro Funzionale di Protezione Civile Regione Marche (Graziano Candelaresi and Franscesca Sini). A special thank comes to Dr. Claudio Mariotti and Dr. Tommaso Moramarco for the precious helps given in the understanding of the hydrological and geological characteristics of the area.

https://doi.org/10.5194/egusphere-2022-340
Preprint. Discussion started: 12 July 2022

References

Abera, W., Formetta, G., Borga, M., and Rigon, R.: Estimating the water budget components and their variability in a pre-alpine basin with JGrass-NewAGE., Advances in water resources, 104, 37–54, https://doi.org/http://dx.doi.org/10.1016/j.advwatres.2017.03.010, 2017.

Addor, N., Newman, A. J., Mizukami, N., and Clark, M. P.: The CAMELS data set: catchment attributes and meteorology for large-sample studies., Hydrology and Earth System Sciences, 21, 5293–5313, 2017.

Bancheri, M., Serafin, F., and Rigon, R.: The representation of hydrological dynamical systems using Extended Petri Nets (EPN)., Water Resources Research, 55, 8895–8921, https://doi.org/http://dx.doi.org/10.1029/2019WR025099, 2019.

Barbetta, S., Coccia, G., Moramarco, T., and Todini, E.: Case Study: A Real-Time Flood Forecasting System with Predictive Uncertainty Estimation for the Godavari River, India., Water, 8, 463, 2016.

Boni, C., Bono, P., and Capelli, G.: Schema idrogeologico dell'Italia Centrale (Hydrogeological scheme of central Italy)., Memorie Della Societa Geologica Italiana, 35, 991–1012, 1986.

Bottazzi, M., Bancheri, M., Mobilia, M., Bertoldi, G., Longobardi, A., and Rigon, R.: Comparing Evapotranspiration Estimates from the GEOframe-Prospero Model with Penman–Monteith and Priestley-Taylor Approaches under Different Climate Conditions., Water, 13, 1221–1242, https://doi.org/https://doi.org/10.3390/w13091221, 2021.

Butscher, C. and Huggenberger, P.: Intrinsic vulnerability assessment in karst areas: A numerical modeling approach., Water Resources Research, 44, 1–15, https://doi.org/http://dx.doi.org/10.1029/2007WR006277, 2008.

Castilla-Rho, J. C., Mariethoz, G., Rojas, R., Andersen, M. S., and Kelly, B. F.: An agent-based platform for simulating complex human–aquifer interactions in managed groundwater systems., Environmental Modelling and Software, 73, 305–323, https://doi.org/http://dx.doi.org/10.1016/j.envsoft.2015.08.018, 2015.

Coccia, G. and Todini, E.: Recent developments in predictive uncertainty assessment based on the model conditional processor approach., Hydrol. Earth Syst. Sci., 15, 3253–3274, 2011.

Di Matteo, L., Dragoni, W., Azzaro, S., Pauselli, C., Porreca, M., Bellina, G., and Cardaci, W.: Effects of earthquakes on the discharge of groundwater systems: The case of the 2016 seismic sequence in the Central Apennines, Italy., Journal of Hydrology, 583, 1–13, https://doi.org/https://doi.org/10.1016/j.jhydrol.2019.124509, 2020.

Di Matteo, L., Capoccioni, A., Porreca, M., and Pauselli, C.: Groundwater-Surface Water Interaction in the Nera River Basin (Central Italy): New Insights after the 2016 Seismic Sequence., Hydrology, 8, 97–114, https://doi.org/https://doi.org/10.3390/hydrology8030097, 2021.

Fan, Y.: Are catchments leaky?, WIREs Water, 6, 1–25, 2019.

Fiorillo, F. and Doglioni, A.: The relation between karst spring discharge and rainfall by cross-correlation analysis (Campania, southern Italy)., Hydrogeology Journal volume, 18, 1881–1895, 2010.

Formetta, G., Kampf, S. K., David, O., and Rigon, R.: Snow water equivalent modeling components in NewAge-JGrass., Geoscientific Model Development, 7, 725–736, https://doi.org/http://dx.doi.org/10.5194/gmd-7-725-2014, 2014.

Fronzi, D., Mirabella, F., Cardellini, C., Caliro, S., Palpacelli, S., Cambi, C., Valigi, D., and Tazioli, A.: The Role of Faults in Groundwater Circulation before and after Seismic Events: Insights from Tracers, Water Isotopes and Geochemistry., Water, 13, 1499–1519, https://doi.org/https://doi.org/10.3390/w13111499, 2021.

Giani, G., Rico-Ramirez, M. A., and Woods, R. A.: A Practical, Objective, and Robust Technique to Directly Estimate Catchment Response Time., Water Resources Research, 57, https://doi.org/https://doi.org/10.1029/2020wr028201, 2021.

https://doi.org/10.5194/egusphere-2022-340
Preprint. Discussion started: 12 July 2022

Gupta, H. V., Kling, H., Yilmaz, K. K., and Martinez, G. F.: Decomposition of the mean squared error and NSE performance criteria: Implications for improving hydrological modelling., J. Hydrol., 377, 80–91, 2009.

Hartmann, A., Goldscheider, N., Wagener, T., Lange, J., and Weiler, M.: Karst water resources in a changing world: Review of hydrological modeling approaches., Reviews of Geophysics, 52, 218–242, 2014.

Hay, L. E., Leavesley, G. H., Clark, M. P., Markstrom, S. L., Viger, R. J., and Umemoto, M.: STEP WISE, MULTIPLE OBJECTIVE CALIBRATION OF A HYDROLOGIC MODEL FOR A SNOWMELT DOMINATED BASIN1., Journal of the American Water Resources Association (JAWRA), 42, 877–890, 2006.

Jukic, D. and Denić-Jukić, V.: Groundwater balance estimation in karst by using a conceptual rainfall-runoff model., Journal of Hydrology, 373, 302–315, 2009.

Kiraly, L., Perrochet, P., and Rossier, Y.: Effect of the epikarst on the hydrograph of karst springs: a numerical approach., Bull. Centre d'Hydrogéol, 14, 199–220, 1995.

Kourgialas, N. N., Karatzas, G. P., and Nikolaidis, N. P.: An integrated framework for the hydrologic simulation of a complex geomorphological river basin., Journal of Hydrology, 381, 308–321, 2010.

Kristoufek, L.: Detrending moving-average cross-correlation coefficient: Measuring cross-correlations between non-stationary series., Physica A: Statistical mechanics and its applications, 406, 169–175, 2014.

Kristoufek, L.: What are the main drivers of the bitcoin price? Evidence from wavelet coherence analysis., PLoS ONE, 28, 1–19, https://doi.org/10.1371/journal.pone. 0123923, 2015.

Lievens, H., Demuzere, M., Marshall, H. P., Reichle, R. H., Brucker, L., Brangers, I., de Rosnay, P., Dumont, M., Girotto, M., Immerzeel, W. W., and Jonas, T.: Snow depth variability in the Northern Hemisphere mountains observed from space., Nature communications, 10, 1–12, https://doi.org/https://www.nature.com/articles/s41467-019-12566-y, 2019.

Massari, C., Maggioni, V., Barbetta, S., Brocca, L., Ciabatta, L., Camici, S., Moramarco, T., Coccia, G., and Todini, E.: Complementing near-real time satellite rainfall products with satellite soil moisture-derived rainfall through a Bayesian Inversion approach., Journal of Hydrology, 573, 341–351, 2019.

Mastrorillo, L., Baldoni, T., Banato, F., Boscherini, A., Cascone, D., Checcucci, R., Petitta, M., and Boni, C.: Analisi idrogeologica quantitativa del dominio carbonatico umbro., Italian Journal of Engineering Geology and Environment, 1, 137–155, 2009.

Mastrorillo, L., Saroli, M., Viaroli, S., Banzato, F., Valigi, D., Petitta, M., Petitta, M., and Boni, C.: Sustained post-seismic effects on groundwater flow in fractured carbonate aquifers in Central Italy., Hydrological Processes, 34, 1167–1181, 2019.

Mazzilli, N., Guinot, V., Jourde, H., Lecoq, N., Labat, D., Arfib, B., Baudement, C., Danquigny, C., Dal Soglio, L., and Bertin, D.: KarstMod: A Modelling Platform for Rainfall - Discharge Analysis and Modelling Dedicated to Karst Systems., Environmental Modelling and Software, 122, 1–10, https://doi.org/http://dx.doi.org/10.1016/j.envsoft.2017.03.015, 2019.

Mu, Q., Zhao, M., and Running, S. W.: MODIS Global Terrestrial Evapotranspiration (ET) Product (NASA MOD16A2/A3) Algorithm Theoretical Basis Document., National Aeronautics and Space Administration, 2013.

Nanni, T., Vivalda, P. M., Palpacelli, S., Marcellini, M., and Tazioli, A.: Groundwater circulation and earthquake-related changes in hydrogeological karst environments: a case study of the Sibillini Mountains (central Italy) involving artificial tracers., Hydrogeology Journal, 28, 2409–2428, https://doi.org/https://doi.org/10.1007/s10040-020-02207-w, 2020.

Rimmer, A. and Hartmann, A.: Simplified Conceptual Structures and Analytical Solutions for Groundwater Discharge Using Reservoir Equations., 2, 217–238, https://doi.org/http://dx.doi.org/10.5772/34803, 2012.

https://doi.org/10.5194/egusphere-2022-340
Preprint. Discussion started: 12 July 2022

Rooji, R. D.: Towards Improved Numerical Modeling of Karst Aquifers: Coupling Turbulent Conduit Flow and Laminar Matrix Flow under Variably Saturated Conditions., Université de Neuchâtel, 583, 1–13, https://doi.org/https://doc.rero.ch/record/8817, 2020.

Schymanski, S. and Or, D.: Leaf-scale experiments reveal an important omission in the Penman-Monteith equation., Hydrol. EarthSyst. Sci., 21, 685–706, 2017.

Tapoglou, E., Karatzas, G. P., Trichakis, I. C., and Varouchakis, E. A.: A spatio-temporal hybrid neural network-Kriging model for groundwater level simulation., Journal of hydrology, 519, 3193–3203, https://doi.org/http://dx.doi.org/10.1016/j.jhydrol.2014.10.040, 2014.

Tritz, S., Guinot, V., and Jourde, H.: Modelling the Behaviour of a Karst System Catchment Using Non-Linear Hysteretic Conceptual Model., Journal of Hydrology, 397, 250–262, https://doi.org/http://dx.doi.org/10.1016/j.jhydrol.2010.12.001, 2011.

Valigi, D., Fronzi, D., Cambi, C., Beddini, G., Cardellini, C., Checcucci, R., Mastrorillo, L., Mirabella, F., and Tazioli, A.: Earthquake-induced spring discharge modifications: The Pescara di Arquata spring reaction to the August–October 2016 Central Italy earthquakes., Water, 12, 1–8, 2020.

Zhang, z., Chen, X., Cheng, Q., and Soulsby, C.: Using Storage Selection (SAS) functions to understand flow paths and age distributions in contrasting karst groundwater systems., Journal of Hydrology, 602, 218–242, 2021.